Relationships between quantitative spinal cord MRI and retinal layers in multiple sclerosis

Jiwon Oh, MD, PhD, FRCPC
Elias S. Sotirchos, MD
Shiv Saidha, MBBCh, MRCPI
Anna Whetstone, BSc
Min Chen, BSc
Scott D. Newsome, DO
Kathy Zackowski, PhD
Laura J. Balcer, MD, MSCE
Elliot Frohman, MD, PhD
Jerry Prince, PhD
Marie Diener-West, PhD
Daniel S. Reich, MD, PhD
Peter A. Calabresi, MD

Correspondence to Dr. Calabresi: pcalabr1@jhmi.edu or Dr. Oh: joh20@jhu.edu

ABSTRACT

Objective: To assess relationships between spinal cord MRI (SC-MRI) and retinal measures, and to evaluate whether these measures independently relate to clinical disability in multiple sclerosis (MS).

Methods: One hundred two patients with MS and 11 healthy controls underwent 3-tesla brain and cervical SC-MRI, which included standard T1- and T2-based sequences and diffusion-tensor and magnetization-transfer imaging, and optical coherence tomography with automated segmentation. Clinical assessments included visual acuity (VA), Expanded Disability Status Scale, MS functional composite, vibration sensation threshold, and hip-flexion strength. Regions of interest circumscribing SC cross-sections at C3-4 were used to obtain cross-sectional area (CSA), fractional anisotropy (FA), perpendicular diffusivity ($\lambda_\perp$), and magnetization transfer ratio. Multivariable regression assessed group differences and SC, retinal, and clinical relationships.

Results: In MS, there were correlations between SC-CSA, SC-FA, SC-$\lambda_\perp$, and peripapillary retinal nerve fiber layer (pRNFL) ($p = 0.01$, $p = 0.002$, $p = 0.001$, respectively) after adjusting for age, sex, prior optic neuritis, and brain atrophy. In multivariable clinical models, when SC-CSA, pRNFL, and brain atrophy were included simultaneously, SC-CSA and pRNFL retained independent relationships with low-contrast VA ($p = 0.04$, $p = 0.002$, respectively), high-contrast VA ($p = 0.06$, $p = 0.008$), and vibration sensation threshold ($p = 0.01$, $p = 0.05$). SC-CSA alone retained independent relationships with Expanded Disability Status Scale ($p = 0.001$), hip-flexion strength ($p = 0.001$), and MS functional composite ($p = 0.004$).

Conclusions: In this cross-sectional study of patients with MS, correlations exist between SC-MRI and retinal layers, and both exhibit independent relationships with clinical dysfunction. These findings suggest that the SC and optic nerve reflect ongoing global pathologic processes that supplement measures of whole-brain atrophy, highlighting the importance of combining measures from unique compartments to facilitate a thorough examination of regional and global disease processes that contribute to clinical disability in MS. *Neurology*® 2015;84:720–728

GLOSSARY

BPF = brain parenchymal fraction; **CSA** = cross-sectional area; **DTI** = diffusion tensor imaging; **DW** = diffusion weighted; **EDSS** = Expanded Disability Status Scale; **FA** = fractional anisotropy; **FOV** = field of view; **GCL** = ganglion cell layer; **HC** = healthy control; **IPL** = inner plexiform layer; **$\lambda_\perp$** = perpendicular diffusivity; **MLR** = multivariable linear regression; **mRNFL** = macular retinal nerve fiber layer; **MS** = multiple sclerosis; **MSFC** = multiple sclerosis functional composite; **MT** = magnetization transfer; **MTR** = magnetization transfer ratio; **OCT** = optical coherence tomography; **PPMS** = primary progressive multiple sclerosis; **pRNFL** = peripapillary retinal nerve fiber layer; **RNFL** = retinal nerve fiber layer; **ROI** = region of interest; **RSEE** = robust standard error estimation; **SC** = spinal cord; **SPMS** = secondary progressive multiple sclerosis; **TE** = echo time; **TI** = inversion time; **TR** = repetition time; **VA** = visual acuity; **VST** = vibration sensation threshold.

Multiple sclerosis (MS) is an immune-mediated disorder that manifests clinically in myriad ways due to lesions involving various regions of the CNS. Visual and sensorimotor dysfunction attributable to optic nerve and spinal cord (SC) lesions are 2 of the most common ways in which patients with MS present,[1,2] and pathologic changes are observed in these structures in the majority of patients, making them important regions to study in MS.[3,4]

Supplemental data at Neurology.org

From the Departments of Neurology (J.O., E.S.S., S.S., A.W., S.D.N., K.Z., D.S.R., P.A.C.), Electrical and Computer Engineering (M.C., J.P.), Computer Science (J.P.), Physical Medicine and Rehabilitation (K.Z.), Biostatistics (M.C., M.D.-W., D.S.R.), and Radiology and Radiological Science (D.S.R.), Johns Hopkins University, Baltimore, MD; Division of Neurology (J.O.), Department of Medicine, St. Michael's Hospital, University of Toronto, Canada; Motion Analysis Laboratory (K.Z.), Kennedy Krieger Institute, Baltimore, MD; Department of Neurology (L.J.B.), University of Pennsylvania School of Medicine, Philadelphia; Departments of Neurology and Ophthalmology (E.F.), University of Texas Southwestern Medical Center at Dallas; and Translational Neuroradiology Unit (D.S.R.), National Institute of Neurological Disorders and Stroke, Bethesda, MD.

Go to Neurology.org for full disclosures. Funding information and disclosures deemed relevant by the authors, if any, are provided at the end of the article.

Several observations raise the possibility of a specific relationship between the optic nerves and SC in MS. Clinical variants of demyelinating disease that predominately affect the optic nerves and SC exist, including opticospinal MS[5] and Devic disease,[6] and myelin oligodendrocyte–induced opticospinal experimental autoimmune encephalitis in mice.[7] To date, relationships between retinal and SC measures in MS have not been assessed, and the degree to which these measures independently relate to clinical disability in MS are unknown.

The objective of this study was to assess relationships among SC-MRI measures, retinal layers, and clinical dysfunction in MS. We hypothesized that correlations between SC-MRI (cross-sectional area [CSA], fractional anisotropy [FA], and magnetization transfer ratio [MTR]) and retinal nerve fiber layer (RNFL) would exist, and that these measures would independently relate to clinical disability in MS. Understanding relationships between tissue damage in distinct CNS compartments is essential to gaining a comprehensive understanding of MS-related pathologic processes and how they mediate both regional clinical disability relevant to the optic nerves and SC (vision and sensorimotor function) and global clinical disability (cognition).

METHODS

Standard protocol approvals, registrations, and patient consents. This study was approved by the institutional review board of Johns Hopkins University. All participants provided written informed consent.

Study participants. Patients with relapsing-remitting MS, secondary progressive MS (SPMS), and primary progressive MS (PPMS) were recruited between 2007 and 2009 from the Johns Hopkins MS Clinic by convenience sampling. MS diagnosis was confirmed by the treating neurologist, according to the 2005 McDonald criteria.[8]

Clinical measures. Within 30 days of MRI, MS functional composite (MSFC) scores were obtained and Expanded Disability Status Scale (EDSS) scores were determined by a neurostatus-certified examiner. Vibration sensation thresholds (VSTs) of the great toes were measured using the Vibratron II (Physitemp, Huron, NJ). To assess strength, 2 maximal efforts of hip flexion were averaged using a Microfet2 dynamometer (Hoggan Industries, West Jordan, UT). Both devices have been validated for use in MS to reliably detect sensorimotor dysfunction.[9] Patients with MS who underwent scanning within the 3 months after a clinical relapse were excluded.

Optical coherence tomography. Retinal imaging was performed bilaterally using spectral-domain Cirrus HD-OCT (model 4000, version 5.0; Carl Zeiss Meditec, Dublin, CA), described in detail previously.[10,11] Peripapillary and macular data were obtained with the Optic Disc Cube 200 × 200 and Macular Cube 512 × 128 protocols, respectively. Experienced technicians performed optical coherence tomography (OCT) scans, which were monitored to ensure reliable fixation. Scans with signal strength <7/10 or artifact were excluded.

Macular cube scans were analyzed in a masked fashion using segmentation software, described previously.[12,13] Briefly, segmentation performed 3-dimensionally identifies the inner limiting membrane, the outer boundaries of the macular RNFL (mRNFL), the inner plexiform layer (IPL), outer plexiform layer, and the inner boundary of the retinal pigment epithelium (figure 1). Thereafter, mRNFL, ganglion cell layer (GCL) + IPL, INL + outer plexiform layer, and outer nuclear layer (including inner and outer photoreceptor segments) thicknesses were calculated in an annulus (inner radius = 0.54 mm; outer radius = 2.4 mm), centered on the fovea. This protocol has demonstrated satisfactory reproducibility in MS and healthy control (HC) subjects.[13]

The OCT in closest temporal proximity to the SC-MRI was selected for analysis (median time difference = 179 days; interquartile range = 0–379).

Cervical SC-MRI. Cervical SC-MRIs were performed on a 3T Achieva scanner (Philips Medical Systems, Best, the Netherlands) using 2-element phased array surface coil reception and body-coil excitation.

"MT [magnetization transfer]-weighted images were acquired using a T2*-weighted, 3D-gradient-echo sequence with a MT-prepulse and a multi-shot echo-planar readout (EPI factor = 3, parallel imaging factor = 2, TR/TE/α = 121 ms/12.5 ms/9°), yielding 30 contiguous 3-mm axial slices spanning vertebral levels C2–C6, nominal in-plane resolution: 0.6 × 0.6 mm^2. Scans were acquired with (MT_{on}) and without (MT_{off}) a 1.5-kHz off-resonance sinc-gauss-shaped radiofrequency saturation pulse. MT_{on} was registered to MT_{off} with a 6-degree-of-freedom, rigid-body module implemented in FLIRT (Oxford Centre for Functional MRI of the Brain's Linear Imaging Registration Tool, Oxford, UK)." MTR was calculated using: $(MT_{off} - MT_{on})/MT_{off}$.

"Diffusion-tensor imaging (DTI) data were obtained using a multislice spin-echo sequence with a single-shot echo-planar readout (parallel imaging factor = 2, TR/TE = 4,727 ms/63 ms). Axial fat-suppressed diffusion-weighted images were obtained in 16 non-coplanar gradient directions with b = 500 s/mm^2, one minimally diffusion weighted (DW) acquisition ($b_0 \sim 33$ s/mm^2), 3-mm slice thickness, nominal in-plane resolution: 1.5 × 1.5 mm^2."

"A sagittal, multi-slice turbo spin-echo (TSE factor: 20, parallel imaging factor: 2) short-tau inversion recovery (STIR) (FOV = 250 mm, acquired resolution: 1 × 1 × 2 mm^3 [AP, FH, RL], TR/TE/TI = 4,227 ms/68 ms/200 ms) was acquired."

"Each DW image was registered to the b = 0 volume using a 6-degree-of-freedom, rigid-body registration implemented in FLIRT using JIST (Java Image Science Toolkit)."[14] The diffusion tensor was calculated and maps of FA, mean diffusivity, and $\lambda_\perp$ were generated. The b = 0 image was deformably registered to MT with resulting information applied to DW images.[15,16] DTI indices were calculated from DT eigenvalues.[17]

To delineate regions of interest (ROIs) outlining the SC axial cross-section, an automated reproducible segmentation protocol was applied to MT_{off} images and transferred to DTI/MTR maps (figure 2).[18] DTI maps from 8 patients and the MTR map from one patient were excluded because of inadequate image quality.

Figure 1 Eye of a healthy control subject

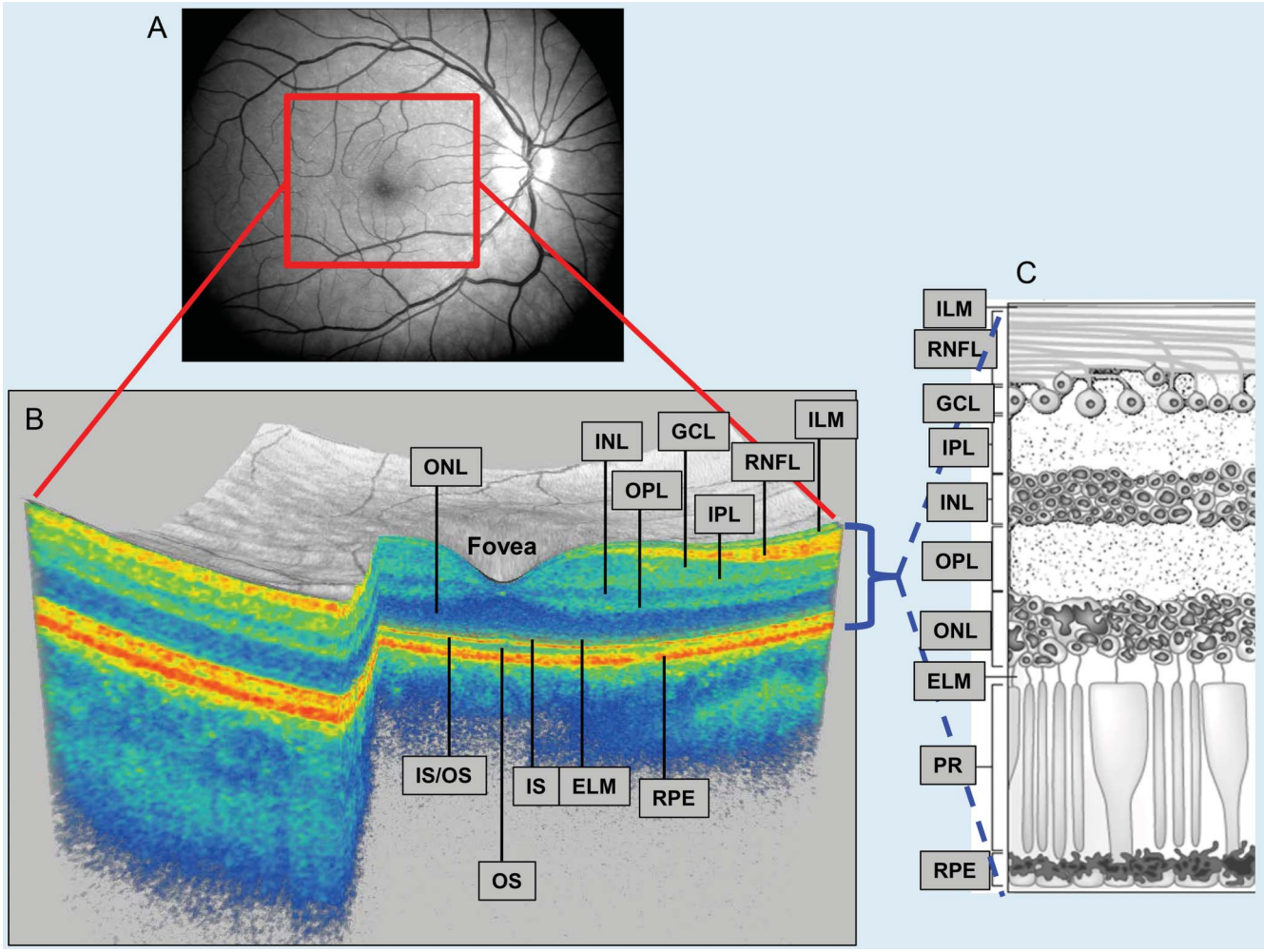

(A) Photograph of fundus. (B) A 3-dimensional macular volume cube generated from the macular region (outlined in red in panel A). Optical coherence tomography segmentation allows determination of retinal layer thicknesses: macular retinal nerve fiber layer (RNFL), GCL + IPL (ganglion cell layer and inner plexiform layer), INL + OPL (inner nuclear layer and outer plexiform layer), and the outer nuclear layer (ONL), which includes the inner and outer photoreceptor segments. Individual retinal layers are readily discernible, but the GCL cannot easily be distinguished from the IPL. (C) Cellular composition of retinal layers. ELM = external limiting membrane; ILM = inner limiting membrane; IS = inner segment; OS = outer segment; PR = photoreceptors; RPE = retinal pigment epithelium.

ROIs were manually adjusted as necessary (MTR/SC-CSA 5% adjusted, DTI maps 40% adjusted). Average values of SC-CSA, FA, $\lambda_{\perp}$, and MTR were calculated using ROIs from C3-4.[14]

Brain MRI. Full details of our brain MRI acquisition have been described previously.[19,20] For this dataset, DTI-based brain volume segmentation had lower scan-to-scan variability than alternate T1-based methods and were used to calculate supratentorial brain and CSF volumes, as previously reported.[20] A recent study similarly found comparable brain substructure segmentations using DTI and T1-based methods.[21] Brain parenchymal fraction (BPF) was calculated as BPF = brain volume/(brain volume + CSF volume).

Statistical analysis. Statistical calculations were performed using STATA version 11 (StataCorp, College Station, TX). Student *t* tests were used to assess group differences in MS vs HCs and relapsing vs progressive MS. Multivariable linear regression (MLR) using robust standard error estimation (RSEE) to account for within-subject, intereye correlations assessed group differences. Because of the exploratory nature of this study and established a priori hypotheses, adjustment for multiple comparisons was not performed,[22] but corrected results are also provided (table e-1 on the *Neurology*® Web site at Neurology.org). Relationships between retinal and SC-MRI measures were assessed using MLR adjusting for potentially confounding covariates of age, sex, BPF, and history of optic neuritis using RSEE. Partial correlations (which need not account for intereye correlations) were calculated for illustrative purposes. Relationships between retinal and SC-MRI measures with clinical disability were assessed using MLR and RSEE with each clinical measure as the dependent variable and SC-CSA, RNFL, age, sex, BPF, and history of optic neuritis included as covariates. SC-CSA and RNFL were chosen as representative SC and retinal measures because they demonstrated the strongest correlations with one another. Statistical significance was defined as $p < 0.05$.

RESULTS This study included 102 patients with MS (66 relapsing-remitting MS, 24 SPMS, 12 PPMS) and 11 HCs. Patients with MS were 69% female,

Figure 2 Automated segmentation of spinal cord cross-sectional area (A, B); color-coded DTI map (C)

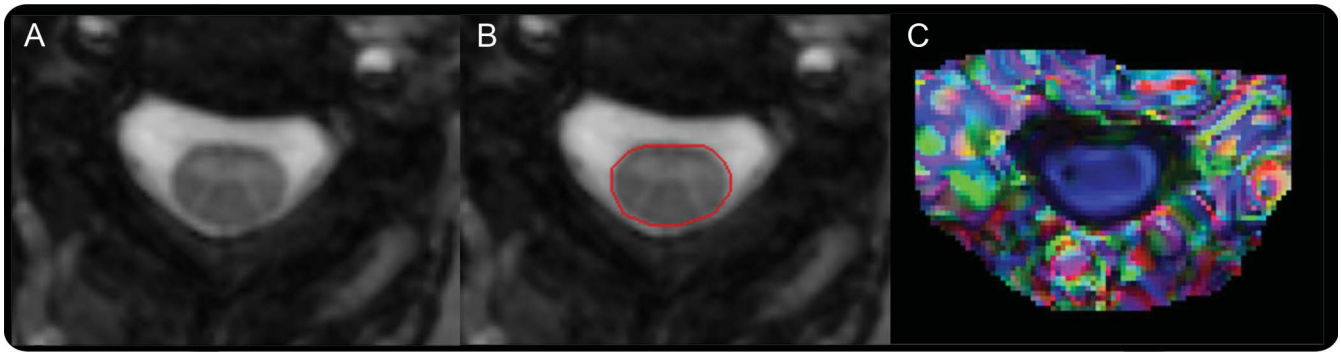

Color-coded diffusion tensor imaging (DTI) map is derived from fractional anisotropy and the principal eigenvector, and demonstrates spinal cord fibers running along the rostrocaudal axis (blue).

had a mean age of 43 years, an average MS disease duration of 9.6 years, and median EDSS score of 3.0. Seventy-one percent of patients with MS were on disease-modifying treatments (table 1).

On assessment of SC-MRI measures, SC-CSA was different between MS vs HCs, while SC-CSA, SC-$\lambda_{\perp}$, and SC-MTR were different between MS subtypes ($p < 0.05$). For retinal layers, peripapillary RNFL (pRNFL), GCL + IPL, and mRNFL were different between MS and HCs ($p < 0.05$), while there were no differences between MS subtypes (table 1).

We established a priori hypotheses regarding specific relationships between SC-MRI and retinal measures, but because this was an exploratory study, we assessed relationships between all available measures. In MS, there were consistently correlations between SC-CSA, SC-FA, SC-$\lambda_{\perp}$, and pRNFL ($p = 0.01$, $p = 0.002$, $p = 0.001$, respectively), mRNFL ($p = 0.007$, $p = 0.03$, $p = 0.04$), and GCL + IPL ($p = 0.003$, $p = 0.003$, $p = 0.01$) after adjusting for age, sex, prior optic neuritis, and BPF. There were no correlations between SC-MRI measures and INL or outer nuclear layer. SC-MRI (CSA, FA, $\lambda_{\perp}$, MTR) and BPF demonstrated univariate correlations ($p < 0.01$ for CSA, FA, MTR; $p = 0.08$ for $\lambda_{\perp}$), but no correlations between SC-MRI and BPF were demonstrated after adjusting for age, sex, retinal measures, and prior optic neuritis ($p > 0.05$ for all comparisons). Univariate correlations between BPF and retinal measures ($r = 0.23$, 0.22, and 0.18 for pRNFL, GCL + IPL, and mRNFL) were smaller than those between SC-CSA and retinal measures ($r = 0.29$, 0.30, and 0.25 for pRNFL, GCL + IPL, and mRNFL).

In HCs, there were no correlations between SC measures (CSA, FA, $\lambda_{\perp}$) and pRNFL, mRNFL, or GCL + IPL, but observed correlations between SC-MTR and GCL + IPL and mRNFL ($p = 0.04$, $p = 0.008$). When correlations between SC and retinal measures were assessed based on MS subtype, they were generally stronger in progressive patients in comparison to patients with relapsing MS (table 2; table e-1 displays results corrected for multiple comparisons).

In multivariable models of clinical dysfunction, when representative SC, retinal, and brain atrophy measures (SC-CSA, pRNFL, and BPF) were included simultaneously with other covariates (age, sex, prior optic neuritis, BPF), SC-CSA and pRNFL retained independent relationships with low-contrast visual acuity (VA) ($p = 0.04$, $p = 0.002$, respectively), high-contrast VA ($p = 0.06$, $p = 0.008$), and VST ($p = 0.01$, $p = 0.05$). SC-CSA alone retained an independent relationship with EDSS ($p = 0.001$) and hip-flexion strength ($p = 0.001$), while SC-CSA and BPF retained independent relationships with MSFC (figure e-1, table 3). Notably, BPF only contributed to explaining clinical variance in MSFC ($p < 0.001$) and high-contrast VA ($p = 0.09$). The inclusion of cervical SC lesion count in the clinical models did not significantly alter these observations (table e-2), nor did the removal of BPF as a covariate (table e-3).

DISCUSSION In this study, we found correlations between quantitative SC-MRI and specific retinal layers in patients with MS, suggesting that pathologic changes in 2 functionally and spatially distinct CNS compartments reflect global pathologic processes that occur across all affected CNS compartments in MS, that may be distinct from, and supplement those captured by brain-atrophy measures. Furthermore, when relationships between SC, retinal, and brain atrophy were assessed with various clinical measures, both retinal and SC-MRI measures simultaneously contributed to explaining the variance in functional system-specific clinical disability of relevance to the visual

Table 1 Clinical characteristics, MRI measures, and retinal measures

	All MS (n = 102, 204 eyes)	RRMS (n = 66, 132 eyes)	Progressive (SPMS and PPMS) (n = 36, 72 eyes)	HCs (n = 11, 22 eyes)	*p* Value (MS vs HCs)	*p* Value (RRMS vs PMS)
Subjects, n	102	66	36	11		
Age at MRI scan, y (SD)	43.0 (11.5)	37.9 (10.2)	52.3 (7.4)	38.5 (8.9)	0.22	<0.001[a]
% Female	68.6	72.7	61.1	72.7	0.78	0.23
Disease duration, y (SD)	9.6 (8.6)	6.5 (5.2)	15.0 (10.6)	NA	NA	<0.001[a]
Median baseline EDSS score (IQR)	3.0 (2–6)	2.5 (1.5–3.5)	6.0 (4.0–6.5)	NA	NA	<0.001[a]
% On disease-modifying treatment	71.3	84.8	47.2	NA	NA	<0.001[a]
Vibration sensation threshold, μm (SD)	14.1 (21.1)	8.0 (13.8)	25.2 (26.9)	NA	NA	<0.001[a]
Hip-flexion strength, lb (SD)	39.3 (18.2)	45.1 (15.7)	28.2 (17.9)	NA	NA	<0.001[a]
% Eyes with history of optic neuritis	24.4	26.0	21.3	NA	NA	0.28
Cord cross-sectional area, mm^2 (SD)	77.3 (8.6)	79.8 (8.0)	72.7 (7.9)	83.3 (9.5)	0.03[a]	<0.001[a]
Lesion count, n (SD)	2.1 (1.5)	1.8 (1.5)	2.6 (1.3)	0	<0.001[a]	0.01[a]
Brain parenchymal fraction (SD)	0.87 (0.05)	0.89 (0.05)	0.84 (0.04)	0.90 (0.05)	0.09	<0.001[a]
FA (SD)	0.61 (0.06)	0.62 (0.06)	0.60 (0.06)	0.64 (0.05)	0.09	0.06
$\lambda_{\perp}$, μm^2/ms (SD)	0.76 (0.16)	0.74 (0.15)	0.81 (0.17)	0.67 (0.10)	0.05	0.03[a]
$\lambda_{\parallel}$, μm^2/ms (SD)	2.24 (0.21)	2.21 (0.20)	2.28 (0.21)	2.16 (0.18)	0.24	0.10
MTR (SD)	0.30 (0.05)	0.31 (0.04)	0.28 (0.05)	0.31 (0.02)	0.31	0.0004[a]
pRNFL, μm (SD)	82.2 (12.2)	83.2 (12.6)	80.5 (11.4)	92.9 (10.3)	0.001[a]	0.22
GCL + IPL, μm (SD)	69.8 (10.1)	70.6 (10.0)	68.4 (10.1)	83.0 (4.7)	<0.001[a]	0.24
mRNFL, μm (SD)	28.4 (5.4)	28.6 (5.6)	28.0 (5.0)	34.4 (3.4)	<0.001[a]	0.55
INL + OPL, μm (SD)	65.2 (4.9)	65.6 (4.8)	64.4 (5.1)	65.4 (5.0)	0.88	0.17
ONL, μm (SD)	119.8 (8.2)	119.1 (7.0)	121.0 (9.8)	120.9 (6.0)	0.56	0.26

Abbreviations: EDSS = Expanded Disability Status Scale; FA = fractional anisotropy; GCL + IPL = ganglion cell layer + inner plexiform layer; HC = healthy control; INL + OPL = inner nuclear layer + outer plexiform layer; IQR = interquartile range; $\lambda_{\parallel}$ = parallel diffusivity; $\lambda_{\perp}$ = perpendicular diffusivity; mRNFL = macular retinal nerve fiber layer; MS = multiple sclerosis; MTR = magnetization transfer ratio; NA = not applicable; ONL = outer nuclear layer; PMS = progressive multiple sclerosis; PPMS = primary progressive multiple sclerosis; pRNFL = peripapillary retinal nerve fiber layer; RRMS = relapsing-remitting multiple sclerosis; SPMS = secondary progressive multiple sclerosis.
Optical coherence tomography comparisons adjusted for between-eye correlation.
[a] *p* Values <0.05.

system and SC, suggesting that MS-related changes in the retina and SC are capturing clinically relevant global pathologic processes that are not adequately captured by either measure alone, or by a measure of brain atrophy.

Disease mechanisms in MS are complex and incompletely understood. Although inflammation is likely a significant driving force behind MS-related pathology in all stages of disease, accumulating evidence suggests that immunopathologic mechanisms of tissue injury and region-specific pathology may be distinct in different disease stages.[23,24]

Considering region-specific pathologic differences, prior studies have found limited correlations between measures of SC and brain atrophy (SC-CSA and BPF), suggesting that pathogenic mechanisms in MS evolve independently to an extent in the brain and SC, particularly in progressive phases of disease, supporting the idea that MS disease mechanisms may differentially affect specific regions of the CNS.[14,25,26] Our observations of moderate correlations between SC and retinal measures, but absent correlations between measures of SC and brain atrophy support the notion that MS disease pathology is nonuniform in distinct CNS compartments,[27,28] and suggest there are clinically relevant pathologic processes occurring in the SC and retina that are distinct from those in the brain. Moreover, our observations of stronger SC and retinal correlations in progressive patients support the view that immunopathologic and tissue injury mechanisms of MS differ by disease subtype, and may be indicative of more uniform pathologic changes occurring in PPMS and SPMS, although these progressive MS subtypes may not be equivalent pathologically. However, it is possible that alternate explanations could account for these observations, including the possibility that measures of atrophy in the brain and SC may not be reflective of equivalent disease processes.

Table 2 Relationships between optical coherence tomography measures and SC-MRI measures in MS

	SC-CSA	SC-FA	SC-$\lambda_{\perp}$	SC-$\lambda_{\parallel}$	SC-MTR
All patients (n = 102)					
pRNFL	0.01[a] (0.23)	0.002[a] (0.28)	0.001[a] (−0.25)	0.18 (−0.12)	0.34 (0.08)
GCL + IPL	0.005[a] (0.24)	0.002[a] (0.29)	0.02[a] (−0.23)	0.70 (−0.04)	0.06 (0.17)
mRNFL	0.007[a] (0.22)	0.03[a] (0.22)	0.04[a] (−0.20)	0.22 (−0.10)	0.24 (0.11)
INL	0.55 (0.06)	0.85 (0.02)	0.94 (−0.007)	0.59 (0.05)	0.45 (0.06)
ONL	0.80 (−0.03)	0.19 (0.14)	0.08 (−0.16)	0.08 (−0.15)	0.34 (0.10)
Relapsing MS (n = 66)					
pRNFL	0.43 (0.09)	0.03[a] (0.25)	0.007[a] (−0.28)	0.01[a] (−0.25)	0.43 (−0.08)
GCL + IPL	0.10 (0.19)	0.03[a] (0.28)	0.03[a] (−0.28)	0.38 (−0.11)	0.67 (0.05)
mRNFL	0.03[a] (0.23)	0.09 (0.21)	0.07 (−0.23)	0.38 (−0.10)	0.97 (0.005)
INL	0.65 (0.06)	0.51 (−0.07)	0.67 (0.05)	0.70 (0.05)	0.26 (0.12)
ONL	0.90 (−0.02)	0.06[a] (0.20)	0.06 (−0.23)	0.05 (−0.24)	0.19 (0.19)
Progressive MS (n = 36)					
pRNFL	0.002[a] (0.44)	0.005[a] (0.39)	0.02[a] (−0.31)	0.70 (0.06)	0.15 (0.21)
GCL + IPL	0.03[a] (0.29)	0.003[a] (0.40)	0.04[a] (−0.28)	0.99 (−0.002)	0.02[a] (0.31)
mRNFL	0.21 (0.14)	0.09 (0.26)	0.12 (−0.24)	0.09 (−0.23)	0.39 (0.14)
INL	0.84 (0.03)	0.15 (0.20)	0.41 (−0.12)	0.73 (0.05)	0.78 (0.03)
ONL	0.91 (−0.01)	0.98 (−0.004)	0.98 (−0.003)	0.96 (0.007)	0.45 (−0.08)
HCs (n = 11)					
pRNFL	0.45 (0.26)	0.19 (0.41)	0.07 (−0.58)	0.25 (−0.32)	0.5 (0.21)
GCL + IPL	0.09 (0.43)	0.81 (−0.10)	0.72 (−0.14)	0.25 (−0.24)	0.04[a] (0.42)
mRNFL	0.13 (−0.34)	0.91 (0.02)	0.67 (−0.06)	0.26 (−0.36)	0.008[a] (0.48)
INL	0.68 (−0.16)	0.18 (−0.43)	0.13 (0.53)	0.24 (0.38)	0.06 (0.49)
ONL	0.87 (−0.06)	0.57 (0.16)	0.35 (−0.32)	0.19 (−0.52)	0.13 (0.44)

Abbreviations: GCL + IPL = ganglion cell layer + inner plexiform layer; HC = healthy control; INL = inner nuclear layer; mRNFL = macular retinal nerve fiber layer; MS = multiple sclerosis; ONL = outer nuclear layer; pRNFL = peripapillary retinal nerve fiber layer; SC-CSA = spinal cord cross-sectional area; SC-FA = spinal cord fractional anisotropy; SC-$\lambda_{\parallel}$ = spinal cord parallel diffusivity; SC-$\lambda_{\perp}$ = spinal cord perpendicular diffusivity; SC-MRI = spinal cord MRI; SC-MTR = spinal cord magnetization transfer ratio.

Data are *p* values (partial correlation coefficients). The *p* values are derived from linear regression using robust standard error estimations to account for intereye correlations, adjusting for age, sex, brain parenchymal fraction, and history of optic neuritis; partial correlation coefficients are presented for illustrative purposes only and represent the magnitude of the correlation between retinal and spinal cord measures adjusted for age, sex, brain parenchymal fraction, and history of optic neuritis, but not accounting for within-subject intereye correlations.

[a] *p* Values <0.05.

Noteworthy is the observation that both retinal and SC atrophy measures independently contributed to explaining variance in VA and VST, both of which are system-specific clinical measures of relevance in the retina and SC, respectively. Our findings expand on prior studies that demonstrated that retinal layers (pRNFL and GCL + IPL) reflect global clinical and radiologic CNS processes in MS, and that specific retinal layers may reflect differential pathologic processes, including neurodegeneration and inflammation.[27,29] Our findings suggest that not only do retinal and SC-MRI measures reflect global pathologic processes in MS that are not adequately captured by brain atrophy alone, but that the regional and global pathologic processes that SC-MRI reflect are distinct from those that are captured by retinal measures, and that these processes independently contribute to mediating clinical disability in various functional systems. These findings highlight the importance of including an assessment of multiple compartments of the CNS affected by MS to better understand both global and regional disease processes, their interplay, and how they contribute to clinical disability in various functional systems.

Among clinical measures, we found that with the inclusion of SC and retinal measures, brain atrophy retained a relationship with only MSFC and high-contrast VA. Brain atrophy is a well-established measure of clinical relevance in MS,[30] which our findings do not undermine. However, the ability of retinal and

Table 3 β Coefficients, *p* values, and r^2 values of multivariable models of clinical dysfunction in all patients with MS (n = 102)

	Clinical models											
	EDSS (r^2 = 0.40)		High-contrast VA (r^2 = 0.18)		Low-contrast VA (r^2 = 0.18)		Vibratron (r^2 = 0.24)		Dynamometry (r^2 = 0.36)		MSFC (r^2 = 0.31)	
	Coefficient (95% CI)	*p* Value	Coefficient (95% CI)	*p* Value	Coefficient (95% CI)	*p* Value	Coefficient (95% CI)	*p* Value	Coefficient (95% CI)	*p* Value	Coefficient (95% CI)	*p* Value
SC-CSA	−0.075 (−0.12, −0.03)	<0.01[a]	0.21 (−0.01, 0.44)	0.06	0.26 (0.02, 0.50)	0.04[a]	−0.65 (−1.2, −0.14)	0.01[a]	0.67 (0.27, 1.1)	<0.01[a]	0.013 (0.004, 0.022)	<0.01[a]
pRNFL	−0.13 (−0.04, 0.02)	0.35	0.20 (0.06, 0.40)	<0.01[a]	0.26 (0.10, 0.43)	<0.01[a]	−0.40 (−0.8, −0.004)	0.05	0.18 (−0.11, 0.46)	0.22	0.00013 (−0.008, 0.008)	0.97
Age	0.074 (0.04, 0.10)	<0.01[a]	0.12 (−0.08, 0.31)	0.23	0.0016 (−0.14, 0.14)	0.98	0.43 (0.06, 0.80)	0.02[a]	−0.51 (−0.79, −0.22)	<0.01[a]	−0.00093 (−0.01, 0.008)	0.84
Sex	0.59 (−0.10, 1.3)	0.09	1.67 (−2.2, 5.5)	0.40	−1.16 (−4.9, 2.6)	0.54	5.88 (−0.51, 12)	0.07	11.9 (4.8, 19)	<0.01[a]	−0.41 (−0.23, 0.15)	0.67
BPF	−2.70 (−10, 5.0)	0.49	41.5 (−6.1, 89)	0.09	−14.8 (−52, 23)	0.44	21.7 (−66, 110)	0.63	−11.8 (−67, 43)	0.67	4.97 (2.7, 7.2)	<0.01[a]
History of ON	−0.46 (−1.2, 0.03)	0.20	−2.81 (−8.5, 2.9)	0.33	−2.75 (−6.5, 1.0)	0.15	−2.13 (−11, 7)	0.65	2.82 (−3.2, 8.8)	0.35	0.041 (−0.16, 0.24)	0.68

Abbreviations: BPF = brain parenchymal fraction; CI = confidence interval; EDSS = Expanded Disability Status Scale; MS = multiple sclerosis; MSFC = multiple sclerosis functional composite; ON = optic neuritis; pRNFL = peripapillary retinal nerve fiber layer; SC-CSA = spinal cord cross-sectional area; VA = visual acuity.
The r^2 values represent percent of total clinical variance explained by all covariates in the model; coefficients are β coefficients of each covariate in the multivariable clinical model.
[a] p Values <0.05.

SC measures to better reflect pathologic changes of relevance to disability is likely attributable to the compact anatomical organization of both regions, resulting in less clinically "silent" tissue in comparison to the whole brain, allowing enhanced detection of microstructural changes that are of clinical relevance both locally and globally. Future studies assessing the relative contribution of measures of gray matter atrophy in the brain with retinal and SC measures will be of interest.

Both SC and retinal measures contributed to explaining clinical variance with measures of VA and VST, whereas SC-CSA alone contributed to explaining clinical variance with EDSS, hip-flexion strength, and MSFC. This observation may be attributable, at least in part, to the differential sensitivity of the SC and retinal measures chosen (SC-CSA and pRNFL) to picking up tissue loss relevant to clinical disability in specific functional systems. For instance, SC-CSA may be a measure that is more adept at picking up tissue loss in the corticospinal tracts, rather than the dorsal columns of the SC, which may partially explain the dominant correlation between measures of lower limb strength and SC-CSA. In addition, differential vulnerabilities of clinically relevant tissue to the particular clinical measure may also account for this observed difference. Prior studies have demonstrated good correlations in the corpus callosum and cerebral hemispheres between axonal density and lesion load, but absent correlations in the SC, suggesting that there may be differential tissue vulnerability to axonal injury in different CNS compartments.[31,32] Because the SC and retinal measures we chose (SC-CSA and pRNFL) in this study specifically assessed for tissue loss, depending on tissue vulnerability to axonal loss of clinically relevant regions in specific clinical systems, the relative contribution of these individual measures to clinical disability may differ substantially. Another factor contributing to these findings may be that the major functional pathways mediating vision and sensation route through the thalamus, which is known to be highly atrophic even in early MS.[33] Thus, SC and retinal atrophy may be relevant to vision and sensation, because they reflect anterograde and retrograde degeneration from primary thalamic pathology. Taken together, these findings further highlight the heterogeneity and complexity of MS disease pathogenesis, and underscore the importance of integrating measures from different regions of the CNS to obtain a more comprehensive view of MS disease effects as specific measures may be more relevant depending on the clinical system under consideration. Moreover, incorporating measures

from different CNS compartments will be of increasing relevance as the tools used to measure disability in MS improve to more accurately reflect the actual clinical burden of disease.

This study has a number of limitations. First, our number of HCs was limited, and many of our subgroup analyses were performed using a relatively small sample size. Notwithstanding this limitation, we were still able to identify consistent relationships between a variety of retinal and SC measures in patients with MS, which lends credence to our findings. However, the small number of HCs likely resulted in the observation of spurious correlations between SC and retinal measures that are of questionable significance, because we would expect a true correlation between retinal and SC measures to be generally consistent across pRNFL, mRNFL, and GCL + IPL. This was not the case with HCs, in contrast to the consistent relationships observed in MS cases with SC measures and pRNFL, mRNFL, and GCL + IPL. Nonetheless, the small number of subjects precludes the formation of definitive conclusions about SC and retinal correlations in HCs, and the possibility of a relationship between these measures in HCs cannot be dismissed until a larger study is performed. Second, we did not adjust for multiple comparisons because this was an exploratory study; however, all analyses were performed with established a priori hypotheses. Third, SC-MRI measures were obtained from a short segment of the SC, but this did not preclude our ability to detect robust correlations with retinal and clinical measures. Fourth, we utilized DTI-based segmentations to measure whole-brain atrophy, because we found that this approach consistently resulted in the least variability in our dataset. However, this technique has not been fully compared with more conventional T1-based segmentation and thus could have influenced the apparent lack of association between brain atrophy and clinical measures. Finally, although SC-MRIs and OCTs were not performed simultaneously in most, this is unlikely to have influenced any of the conclusions that we derived from our observations. Theoretically, the time lag could possibly have weakened some of the relationships observed, but that we were able to demonstrate consistent correlations suggests that these findings are robust, and worthy of further exploration.

Our findings illustrate that SC and retinal measures supplement the information captured by measures of brain atrophy regarding ongoing global pathologic processes of relevance to a spectrum of disability measures in MS. These findings highlight the importance of combining measures from unique compartments of the CNS to facilitate a more thorough examination of regional and global disease processes that contribute to clinical disability in MS. Further studies in prospective, larger sample sizes of patients with MS and HCs are needed to confirm these findings and to assess how the combination of SC, retinal, and brain measures relate to clinical disability progression. With prospective confirmation, this approach not only has the potential to be of significant clinical utility, but may substantially enhance our understanding of the evolution of disease processes in MS.

AUTHOR CONTRIBUTIONS

Conceptualization of the study: Jiwon Oh, Peter A. Calabresi. Pulse sequence design/implementation and quality control: Daniel S. Reich, Min Chen, Jerry Prince. Analysis/interpretation of the data: Jiwon Oh, Elias Sotirchos, Daniel S. Reich, Peter A. Calabresi. Statistical analysis: Jiwon Oh (Department of Neurology, Johns Hopkins University), Marie Diener-West (Department of Biostatistics, Johns Hopkins University). Drafting/revising the manuscript: Jiwon Oh, Elias S. Sotirchos, Shiv Saidha, Anna Whetstone, Min Chen, Scott D. Newsome, Kathy Zackowski, Jerry Prince, Marie Diener-West, Daniel S. Reich, Peter A. Calabresi.

STUDY FUNDING

Multiple Sclerosis Society of Canada Transitional Career Development Award (to J.O.), NIH R01NS08234 R01 NS082347 to P.A.C., NIH K01 HDO49476 to K.Z., Intramural Research Program of the National Institute of Neurological Disorders and Stroke (to D.S.R.).

DISCLOSURE

J. Oh has received personal compensation for consulting or speaking from EMD-Serono, Genzyme, Biogen-Idec, and Novartis. E. Sotirchos reports no disclosures relevant to the manuscript. S. Saidha has received personal compensation for consulting from Medical Logix for the development of continuing medical education programs, and has received educational grant support from Teva Neurosciences and Novartis. A. Whetstone and M. Chen report no disclosures relevant to the manuscript. S. Newsome has received personal compensation for consulting from Biogen-Idec and Genzyme. K. Zackowski reports no disclosures relevant to the manuscript. L. Balcer has received consulting fees from Biogen-Idec, Vaccinex, and Genzyme, and has been on a clinical trial advisory board for Biogen-Idec. E. Frohman has received personal compensation for speaking and consulting from Novartis, Genzyme, Acorda, and Teva. J. Prince has received consulting fees and holds stock in Diagnosoft, Inc. M. Diener-West and D. Reich report no disclosures relevant to the manuscript. P. Calabresi has received personal compensation for consulting and serving on scientific advisory boards from Vertex, Abbott, and MedImmune, and has received research funding from Biogen-Idec, Abbott, Vertex, Novartis, and Bayer. Go to Neurology.org for full disclosures.

Received March 25, 2014. Accepted in final form October 28, 2014.

REFERENCES

1. Balcer LJ. Clinical practice: optic neuritis. N Engl J Med 2006;354:1273–1280.
2. Nijeholt GJ, Bergers E, Kamphorst W, et al. Post-mortem high-resolution MRI of the spinal cord in multiple sclerosis: a correlative study with conventional MRI, histopathology and clinical phenotype. Brain 2001; 124:154–166.
3. Bot JC, Blezer EL, Kamphorst W, et al. The spinal cord in multiple sclerosis: relationship of high-spatial-resolution quantitative MR imaging findings to histopathologic results. Radiology 2004;233:531–540.
4. Toussaint D, Perier O, Verstappen A, Bervoets S. Clinicopathological study of the visual pathways, eyes, and

cerebral hemispheres in 32 cases of disseminated sclerosis. J Clin Neuroophthalmol 1983;3:211–220.
5. Kira J. Neuromyelitis optica and Asian phenotype of multiple sclerosis. Ann NY Acad Sci 2008;1142:58–71.
6. Wingerchuk DM, Hogancamp WF, O'Brien PC, Weinshenker BG. The clinical course of neuromyelitis optica (Devic's syndrome). Neurology 1999;53:1107–1114.
7. Bettelli E, Baeten D, Jager A, Sobel RA, Kuchroo VK. Myelin oligodendrocyte glycoprotein-specific T and B cells cooperate to induce a Devic-like disease in mice. J Clin Invest 2006;116:2393–2402.
8. Polman CH, Reingold SC, Edan G, et al. Diagnostic criteria for multiple sclerosis: 2005 revisions to the "McDonald Criteria." Ann Neurol 2005;58:840–846.
9. Newsome SD, Wang JI, Kang JY, Calabresi PA, Zackowski KM. Quantitative measures detect sensory and motor impairments in multiple sclerosis. J Neurol Sci 2011;305:103–111.
10. Syc SB, Warner CV, Hiremath GS, et al. Reproducibility of high-resolution optical coherence tomography in multiple sclerosis. Mult Scler 2010;16:829–839.
11. Warner CV, Syc SB, Stankiewicz AM, et al. The impact of utilizing different optical coherence tomography devices for clinical purposes and in multiple sclerosis trials. PLoS One 2011;6:e22947.
12. Saidha S, Syc SB, Durbin MK, et al. Visual dysfunction in multiple sclerosis correlates better with optical coherence tomography derived estimates of macular ganglion cell layer thickness than peripapillary retinal nerve fiber layer thickness. Mult Scler 2011;17:1449–1463.
13. Saidha S, Syc SB, Ibrahim MA, et al. Primary retinal pathology in multiple sclerosis as detected by optical coherence tomography. Brain 2011;134:518–533.
14. Oh J, Zackowski K, Chen M, et al. Multiparametric MRI correlates of sensorimotor function in the spinal cord in multiple sclerosis. Mult Scler 2013;19:427–435.
15. Rohde GK, Aldroubi A, Dawant BM. The adaptive bases algorithm for intensity-based nonrigid image registration. IEEE Trans Med Imaging 2003;22:1470–1479.
16. Chen MCA, Wheeler MB, Liu X, Prince JL. Multichannel enhancement of the adaptive bases algorithm. Presented at the 16th Annual Meeting of the Organization for Human Brain Mapping; June 6–10, 2010; Barcelona.
17. Smith SA, Jones CK, Gifford A, et al. Reproducibility of tract-specific magnetization transfer and diffusion tensor imaging in the cervical spinal cord at 3 tesla. NMR Biomed 2010;23:207–217.
18. Chen M, Carass A, Oh J, et al. Automatic magnetic resonance spinal cord segmentation with topology constraints for variable fields of view. Neuroimage 2013;83:1051–1062.
19. Reich DS, Smith SA, Zackowski KM, et al. Multiparametric magnetic resonance imaging analysis of the corticospinal tract in multiple sclerosis. Neuroimage 2007;38:271–279.
20. Harrison DM, Caffo BS, Shiee N, et al. Longitudinal changes in diffusion tensor-based quantitative MRI in multiple sclerosis. Neurology 2011;76:179–186.
21. Hasan KM, Moeller FG, Narayana P. DTI-based segmentation and quantification of human brain lateral ventricular CSF volumetry and mean diffusivity: validation, age, gender effects and biophysical implications. Magn Reson Imaging 2014;32:405–412.
22. Bender R, Lange S. Adjusting for multiple testing: when and how? J Clin Epidemiol 2001;54:343–349.
23. Lassmann H, Bruck W, Lucchinetti C. Heterogeneity of multiple sclerosis pathogenesis: implications for diagnosis and therapy. Trends Mol Med 2001;7:115–121.
24. Lucchinetti C, Bruck W, Parisi J, Scheithauer B, Rodriguez M, Lassmann H. Heterogeneity of multiple sclerosis lesions: implications for the pathogenesis of demyelination. Ann Neurol 2000;47:707–717.
25. Cohen AB, Neema M, Arora A, et al. The relationships among MRI-defined spinal cord involvement, brain involvement, and disability in multiple sclerosis. J Neuroimaging 2012;22:122–128.
26. Agosta F, Absinta M, Sormani MP, et al. In vivo assessment of cervical cord damage in MS patients: a longitudinal diffusion tensor MRI study. Brain 2007;130:2211–2219.
27. Saidha S, Sotirchos ES, Oh J, et al. Relationships between retinal axonal and neuronal measures and global central nervous system pathology in multiple sclerosis. JAMA Neurol 2013;70:34–43.
28. Zimmermann H, Freing A, Kaufhold F, et al. Optic neuritis interferes with optical coherence tomography and magnetic resonance imaging correlations. Mult Scler 2013;19:443–450.
29. Ratchford JN, Saidha S, Sotirchos ES, et al. Active MS is associated with accelerated retinal ganglion cell/inner plexiform layer thinning. Neurology 2013;80:47–54.
30. Fisher E, Rudick RA, Cutter G, et al. Relationship between brain atrophy and disability: an 8-year follow-up study of multiple sclerosis patients. Mult Scler 2000;6:373–377.
31. DeLuca GC, Williams K, Evangelou N, Ebers GC, Esiri MM. The contribution of demyelination to axonal loss in multiple sclerosis. Brain 2006;129:1507–1516.
32. Evangelou N, Esiri MM, Smith S, Palace J, Matthews PM. Quantitative pathological evidence for axonal loss in normal appearing white matter in multiple sclerosis. Ann Neurol 2000;47:391–395.
33. Bergsland N, Horakova D, Dwyer MG, et al. Subcortical and cortical gray matter atrophy in a large sample of patients with clinically isolated syndrome and early relapsing-remitting multiple sclerosis. AJNR Am J Neuroradiol 2012;33:1573–1578.